U.S. Department of Veterans Affairs
Public Access Author manuscript
J Invest Dermatol. Author manuscript; available in PMC 2024 April 01.

Published in final edited form as:
J Invest Dermatol. 2023 April ; 143(4): 621–629.e6. doi:10.1016/j.jid.2022.09.658.

FZD6 Promotes Melanoma Cell Invasion but Not Proliferation by Regulating Canonical Wnt Signaling and Epithelial-Mesenchymal Transition

Bo Dong[1,2], **Laura Simonson**[1], **Samantha Vold**[1], **Ethan Oldham**[1], **Lillian Barten**[1], **Nihal Ahmad**[1,3], **Hao Chang**[1,2,3]

[1]Department of Dermatology, The School of Medicine and Public Health, University of Wisconsin-Madison, Madison, Wisconsin, USA

[2]Program in Genetics, University of Wisconsin-Madison, Madison, Wisconsin, USA

[3]William S. Middleton Memorial Veterans Hospital, Madison, Wisconsin, USA

Abstract

FZD6 is a key gene that controls tissue polarity during development. Increasing evidence suggests that it also plays active roles in various cancers. In this study, we show that *FZD6* is overexpressed in multiple melanoma cell lines and human samples. Knockdown or knockout of *FZD6* does not affect cell proliferation but significantly reduces the invasive ability of melanoma cells. In addition, we have found that knockout of *Fzd6* dramatically reduces lung metastasis in the *Pten/BRaf* mouse model of melanoma. Mechanistic studies in vitro and in vivo reveal a surprising involvement of canonical Wnt signaling and epithelial-mesenchymal pathway in the FZD6-mediated invasive phenotype. Together, our study supports a promoter role of FZD6 in melanoma progression.

INTRODUCTION

Melanoma accounts for only about 1% of skin cancers, but it is the leading cause of skin cancer deaths. Despite recent groundbreaking progress in melanoma therapeutics, including BRAF and MAPK/extracellular signal-regulated kinase kinase inhibitors and mAbs against immune check-points, the prognosis remains very poor in almost half of the patients owing to the development of drug resistance, the rapid distant metastasis, and a variety

Correspondence: Hao Chang, Department of Dermatology, The School of Medicine and Public Health, University of Wisconsin-Madison, 7407 WIMR2, 1111 Highland Avenue, Madison, Wisconsin 53705, USA. hchang@dermatology.wisc.edu.

AUTHOR CONTRIBUTIONS

Conceptualization: BD, HC; Data Curation: BD, LS, SV, EO, LB, HC; Formal Analysis: BD, HC; Funding Acquisition: NA, HC; Investigation: BD, LS, SV, EO, LB, HC; Methodology: BD, NA, HC; Project Administration: HC; Resources: NA, HC; Supervision: HC; Validation: BD, LS, HC; Visualization: BD, HC; Writing – Original Draft Preparation: BD, HC; Writing – Review and Editing: BD, LS, SV, EO, LB, NA, HC.

SUPPLEMENTARY MATERIAL

Supplementary material is linked to the online version of the paper at www.jidonline.org, and at https://doi.org/10.1016/j.jid.2022.09.658.

CONFLICT OF INTEREST

The authors state no conflict of interest.

of autoimmune side effects (Larkin et al., 2014; Marconcini et al., 2018; Robert et al., 2015; Russo et al., 2018). A broader understanding of the biology of melanoma, especially how tumor cells metastasize, is needed for developing novel and effective treatments.

The planar cell polarity (PCP) pathway controls tissue polarity during development by regulating the directional movement of cells and coordinating cells to the tissue axes (Goodrich and Strutt, 2011). Recent evidence suggests that PCP is also involved in cancers by promoting tumor cell migration and invasion (Daulat and Borg, 2017; Davey and Moens, 2017; Luga et al., 2012;VanderVorst et al., 2019, 2018). Although significant progress has been made regarding the role of PCP genes in certain cancers, their involvement in melanoma has not been studied.

FZD6 (Fzd6 in mice) is a core frizzled family PCP protein that regulates skin patterning during development (Wang et al., 2016a). In this study, we have found that FZD6 is overexpressed in multiple melanoma cell lines and human tissues. Knockdown or knockout (KO) of *FZD6* does not affect cell proliferation but significantly reduces the invasive ability of melanoma cells in vitro. In addition, we have found that KO of *Fzd6* dramatically inhibits the distant metastasis of melanoma to the lungs in the *Pten/BRaf* mouse model. Furthermore, our in vitro and in vivo experiments strongly suggest that FZD6 promotes melanoma invasion and metastasis by regulating the canonical Wnt signaling and epithelial-mesenchymal transition (EMT) pathways. These findings reveal a critical role of FZD6 in promoting melanoma cell invasion and metastasis.

RESULTS

Expression of *FZD6* and other PCP genes is misregulated in melanoma

We first assessed the expression of *FZD6* and other PCP genes in melanoma cell lines by RT-qPCR. All seven melanoma cell lines (WM35, WM115, 451Lu, A375, G361, Hs294T, and SK-Mel28) had a significantly higher expression of *FZD6* than normal melanocytes (Figure 1a). *FZD3*, a closely related frizzled family gene to *FZD6*, has been shown to promote cell proliferation and metastasis in patient-derived melanoma cells (Li et al., 2019). Its expression was also upregulated in all the seven melanoma cell lines examined. In contrast to a universal upregulation of *FZD6* and *FZD3*, we observed that the expression changes of the other two PCP family genes, *CELSR1* and *VANGL2*, were variable among melanoma cell lines. *CESLR1* expression was upregulated in A375, G361, SK-Mel28, and WM115. *VANGL2* expression was upregulated in G361, WM35, and WM115 but downregulated in A375, Hs294T, and SK-Mel28 cells. These results suggest that PCP family genes might play various roles in melanoma.

We validated the expression of FZD6 in melanoma cell lines by western blot. Low level of FZD6 protein was detected in normal and immortalized melanocytes, but significantly higher protein levels were found in melanoma cell lines (Figure 1b). We also determined the expression of FZD6 using a human melanoma tissue microarray containing benign nevus and malignant melanoma tissues. We found a significantly higher expression of FZD6 in melanoma tissues than in benign (Figure 1c). Details on the tissue microarray and stained images are provided in Supplementary Table S1 and Supplementary Figure S1.

Knockdown or KO of *FZD6* impairs melanoma cell invasion in vitro

We next determined *FZD6* function in melanoma cells using small interfering RNA knockdown. FZD6 small interfering RNA treatment caused a nearly complete loss of FZD6 proteins in A375 and Hs294T cells (Figure 1d). Knockdown of *FZD6* did not affect cell proliferation, as assessed by CellTiter proliferation assay and cell cycle analysis (Figure 1e and f). We assessed melanoma cell motility using the Matrigel invasion assay and found that significantly fewer cells were able to invade through the Matrigel layer after *FZD6* knockdown (Figure 1g). We also performed a spheroid invasion assay in Hs294T cells and found that *FZD6* knockdown significantly inhibited melanoma cell invasion (Figure 1h).

To achieve a complete deletion of FZD6 in melanoma cells, we generated *FZD6*-KO A375 cell lines using a previously described method (Ran et al., 2013). Two single-guide RNA sequences were used to increase the efficiency of gene disruption (Figure 2a). Five KO clones with a complete loss of FZD6 expression were established (Figure 2b). Four of five clones showed no difference in proliferation compared with the control cells (clone 1 proliferated ~20% faster) (Figure 2c). We performed the Matrigel invasion assay and found that tumor cell invasion in all five KO clones was significantly impaired (Figure 2d). These data suggest that FZD6 is not required for cell survival but promotes the invasiveness of melanoma cells in vitro.

FZD6 overexpression does not affect cell proliferation and invasion in melanocytes

Next, we overexpressed FZD6 in the immortalized melanocyte line, MEL-ST, in which the endogenous expression of FZD6 was barely detectable (Figure 3a). Ectopic FZD6 expression in MEL-ST cells did not affect cell proliferation (Figure 3b and c). We used the Matrigel invasion assay to determine the effect of forced FZD6 expression on cell invasion. MEL-ST cells had low invasion capacity because cells were only found to be able to migrate through the Matrigel occasionally. Overexpression of FZD6 did not enhance the cell invasion in MEL-ST cells (Figure 3d). These results suggest that FZD6 is not sufficient to drive the cell invasiveness in melanocytes, and malignant transformation is probably required for the FZD6-induced cell invasion.

FZD6 regulates canonical Wnt signaling and EMT pathways in melanoma cells

Frizzled receptors can transduce both the canonical Wnt and noncanonical PCP signaling (Nusse and Clevers, 2017; Wang et al., 2016a). To determine whether FZD6 promotes melanoma cell invasion by regulating the PCP pathway, we measured the activation of small Rho family GTPases (Rac1, RhoA, and Cdc42) in A375 cells. High levels of activated RhoA and Cdc42 were detected, but there was no difference between the control and *FZD6*-knockdown A375 cells (Figure 4a). No Rac1 activation was detected. These data suggested that small GTPases are not involved in the FZD6-induced melanoma invasiveness. To determine whether FZD6 promotes melanoma cell invasion by regulating the canonical Wnt signaling, we examined the expression of several canonical Wnt-target genes by qRT-PCR. We found that the expression levels of *CTNNB1*, *AXIN2*, *LEF1*, and *TCF4* were significantly lower in the *FZD6*-knockdown A375 cells, suggesting a decreased canonical Wnt signaling during *FZD6* knockdown (Figure 4b). We also examined the total and active (nonphosphorylated) β-catenin levels in the *FZD6*-knockdown and *FZD6*-KO melanoma

cells by western blot. We found that total and active β-catenin levels significantly reduced during *FZD6* knockdown/KO (Figure 4c). Interestingly, phosphorylation of glycogen synthase kinase 3α/β was not affected by *FZD6* knockdown/KO. We did observe a slightly but significantly increased level of total glycogen synthase kinase 3α/β in *FZD6*-knockdown Hs294T cells but not in A375 cells. On the contrary, we observed a lower level of total glycogen synthase kinase 3α in *FZD6*-KO A375 cells. It remains unclear how much the glycogen synthase kinase activity change contributed to the reduced β-catenin levels in *FZD6*-knockdown/-KO melanoma cells.

EMT is commonly associated with tumor invasion and metastasis in many cancers, including melanoma (Brabletz et al., 2018; Caramel et al., 2013; Hanahan and Weinberg, 2011; White and Zon, 2008). We compared the expression levels of several EMT markers between the control and *FZD6*-knockdown A375 melanoma cells by qRT-PCR (Figure 4d). We found a significantly decreased expression of the mesenchymal markers *CDH2* and *VIM* and the EMT transcriptional regulators *ZEB1* and *ZEB2* upon *FZD6* knockdown. To further examine the effects of FZD6 on EMT in a nonbiased way, we employed a Qiagen RT^2 Profiler PCR Array to determine the transcriptional changes of 84 EMT-related genes upon *FZD6* knockdown (Figure 4e; the original Ct values were plotted in Supplementary Figure S2). Our analysis identified 57 differentially expressed EMT genes. The top upregulated and downregulated genes were *COL3A1* and *CTNNB1*, respectively. Together, these results suggest that FZD6 promotes melanoma cell invasion by regulating the canonical Wnt signaling and EMT.

WNT5A and WNT10B act as potential FZD6 ligands in promoting melanoma invasion

The fact that we observed a phenotype in *FZD6*-knockdown/KO melanoma cells suggests that the ligand of FZD6 is present in the culture media, most likely secreted by the melanoma cells. To determine which WNT ligands are involved in the FZD6-mediated cell invasion in melanoma, we examined the expression of all the 19 WNTs in A375 and Hs294T cells by RT-PCR (Figure 5a) and found that *WNT5A* and *WNT10B* were highly expressed in both cell lines. We knocked down *WNT5A* and *WNT10B* in A375 and Hs294T cells using small interfering RNA. *WNT5A* knockdown caused a slight reduction in cell proliferation in Hs294T cells, whereas *WNT10B* knockdown did not affect cell proliferation in either cell line (Figure 5b). We performed the Matrigel invasion assay and found that melanoma cell invasion was significantly impaired after *WNT5A* and *WNT10B* knockdown (Figure 5c). We examined the expression of several canonical Wnt-target genes and EMT markers by qRT-PCR and found that the expression of these genes was significantly downregulated upon *WNT5A* and *WNT10B* knockdown (Figure 5d). The similar phenotype between *WNT5A/10B* and *FZD6* knockdown and shared mechanisms suggest that WNT5A and WNT10B are potential FZD6 ligands in promoting melanoma invasion.

Wnt5a can act through both frizzled receptors and ROR2 and cause different signaling outputs (Mikels and Nusse, 2006). To determine whether ROR2 is involved in melanoma cell invasion in A375 and Hs294T cells, we examined its expression by western blot. Low and no significant ROR2 proteins were detected in A375 and Hs294T cells, respectively (Figure 5e). The expression level of ROR2 was not affected by *FZD6*, *WNT5A*, or

WNT10B knockdown. It has been reported that WNT5A overexpression in human melanoma cell line UACC 1273 promotes cell motility and invasion by activating protein kinase C (PKC) (Weeraratna et al., 2002). To determine whether PKC is involved in melanoma cell invasion in A375 and Hs294T cells, we monitored the PKC activation and found that the level of phosphorylated PKC was not affected by *FZD6*, *WNT5A*, or *WNT10B* knockdown (Figure 5e). These data suggest that ROR2 and PKC are not involved in the invasive phenotype of A375 and Hs294T melanoma cells.

Fzd6 KO inhibits distant metastasis of melanoma into the lung in mice

We further investigated the role of FZD6 in melanoma using a well-established mouse model, in which tamoxifen-inducible Cre recombinase is targeted to melanocytes to delete the *Pten* gene and turn on the expression of an oncogenic *BRaf* allele (referred to as the *Pten/BRaf* model) (Dankort et al., 2009). Melanomas from this *Pten/BRaf* model expressed high levels of FZD6 proteins (Figure 6a). We crossed the *Pten/BRaf* model to the $Fzd6^{-/-}$ background (Guo et al., 2004) and generated $Tyr\text{-}CreER^{T2};Pten^{loxP/loxP}$; $BRaf^{CA/+};Fzd6^{+/+}$ mice (referred to as the *Pten/BRaf Fzd6* wild type) and $Tyr\text{-}CreER^{T2};Pten^{loxP/loxP};BRaf^{CA/+};Fzd6^{-/-}$ mice (referred to as the *Pten/BRaf Fzd6* KO). We applied 4-hydroxytamoxifen onto the skin (paws, ears, and tail base) of mice aged 4–5 weeks and observed the mice for tumor development (Figure 6b). As reported previously, we also observed that melanoma initiation and progression in the *Pten/BRaf* model were more severe in female mice than in males (Zhai et al., 2020). Thus, we used female mice for our phenotypic analysis. *Pten/BRaf Fzd6*-KO and *Pten/BRaf Fzd6* wild-type mice developed similar skin melanomas after 4-hydroxytamoxifen administration, suggesting that FZD6 does not affect the growth of primary tumors (Figure 6c). To determine whether FZD6 affects melanoma metastasis, we established a cohort of five *Pten/BRaf Fzd6* wild-type and five *Pten/BRaf Fzd6* KO mice and killed the mice 8 weeks after 4-hydroxytamoxifen administration. Lung tissue was examined because it is the most common site of metastasis in the *Pten/BRaf* model. All the five *Pten/BRaf Fzd6* wild-type mice had various macroscopic tumor nodules in the lung. Metastatic tumors appeared to be amelanotic, although melanomas in the skin contained both pigmented and amelanotic melanoma cells. Strikingly, we found that all the five *Pten/BRaf Fzd6*-KO mice were completely free of lung metastases, as verified by histological sections (Figure 6c-e). These results suggest that FZD6 is not required for primary tumor formation and growth, but it promotes melanoma metastasis.

To test whether FZD6 also regulates canonical Wnt signaling and EMT pathways in the *Pten/BRaf* melanoma model, we collected RNA from the primary skin tumors and performed qRT-PCR on several marker genes (Figure 6f). We found a significant downregulation in canonical Wnt signaling (*Ctnnb1*) and EMT (*Cdh2, Snai1/2, Zeb1/2*) genes in the *Fzd6*-KO melanomas. Interestingly, the expression of MITF, the master regulator of melanocyte differentiation, was upregulated in the *Fzd6*-KO melanomas. The results from the *Pten/BRaf* mouse model align with cell culture observations and strongly suggest that FZD6 promotes melanoma invasion and metastasis by regulating the canonical Wnt signaling and EMT.

DISCUSSION

Frizzleds are Wnt receptors that couple to three distinct downstream pathways: the canonical Wnt pathway, the noncanonical PCP pathway, and a less-studied calcium pathway (Wang et al., 2016a). The activation of the canonical Wnt pathway involves the inhibition of β-catenin degradation complex, resulting in the nuclear translocation of β-catenin to regulate transcription (MacDonald et al., 2009; Nusse and Clevers, 2017). The noncanonical PCP pathway controls the asymmetrical localization of PCP protein complexes (Goodrich and Strutt, 2011). Frizzled-induced activation of the canonical and PCP signaling pathways can be monitored using the Super Top-Flash cell line that carries a LEF/TCF luciferase reporter and by detecting the coassembly of Frizzleds with CELSR1 on the cell membrane, respectively (Xu et al., 2004; Yu et al., 2012). FZD6 shows robust colocalization with CELSR1 in MDCK cells but does not activate canonical Wnt signaling when cotransfected with many Wnts in Super Top-Flash cells, suggesting that FZD6 functions mainly through the PCP pathway (Yu et al., 2012). In this study, we observed that knockdown and KO of *FZD6* in melanoma cells caused a significant downregulation of several canonical Wnt-target genes, suggesting that FZD6 can transduce the canonical Wnt signaling. It has been reported that direct manipulation of the canonical Wnt signaling in the *Pten/BRaf* mouse model by β-catenin deletion or stabilization can inhibit or accelerate melanoma metastasis, respectively (Damsky et al., 2011). Interestingly, these changes in metastasis caused by altered canonical Wnt signaling are tightly linked to cell proliferation, which has not been observed in our studies. We focus on the Wnt signaling and EMT in this study, but future nonbiased approaches should provide broader insight into the mechanism of FZD6 in melanoma invasion and metastasis.

The proinvasion role of FZD6 in melanoma that we have identified in this study is consistent with that in a previous study in breast cancer (Corda et al., 2017). Knockdown of *FZD6* causes a significant reduction in the invasive potential of several breast cancer cell lines without affecting cell proliferation. Although it is unknown whether the canonical Wnt signaling or EMT pathway is involved in breast cancer cells, reduced Rho activation and fibronectin deposition have been found during *FZD6* knockdown, suggesting that the noncanonical PCP pathway is involved in the FZD6-induced phenotype in breast cancer cells (Corda et al., 2017). The phenotypic similarities and mechanistic differences of FZD6 inhibition in breast cancer and melanoma strongly suggest that the biological context and particular combination with Wnt ligands might determine which downstream pathway FZD6 activates.

FZD3 is a closely related member of FZD6. Similar to FZD6, FZD3 has also been considered a noncanonical PCP receptor (Wang et al., 2016a; Yu et al., 2012). Because of the functional similarity in tissue polarity, *Fzd3* and *Fzd6* play redundant roles during several developmental processes (Dong et al., 2018; Wang et al., 2016b, 2006). The role of FZD3 has also been studied in melanoma because FZD3 overexpression is found in ~20% of human patient samples (Siemers et al., 2017). Experiments using patient-derived melanoma cells have shown that *FZD3* plays a critical role in regulating cell proliferation and that the knockdown of *FZD3* in these cells reduces melanoma growth and progression when engrafted into NOD scid gamma mice (Li et al., 2019). Although both *FZD3* and

FZD6 are overexpressed in melanoma and appear to play a procancer role, there are at least three distinct differences between them. First, FZD3 is required for cell survival, whereas FZD6 is not. Second, FZD6 promotes melanoma progression and metastasis by regulating cell invasiveness, whereas FZD3 promotes it by regulating cell proliferation. Third, FZD6 regulates canonical Wnt signaling and EMT in melanoma, whereas FZD3 promotes melanoma cell proliferation independent of the canonical Wnt signaling. These differences highlight the functional specificity of FZD3 and FZD6 in cancer despite a significant similarity in their role in development.

MATERIALS AND METHODS

Mouse lines

Tyr-CreER^{T2};Pten$^{loxP/loxP}$;BRaf$^{CA/+}$ mice (Dankort et al., 2009) were purchased from the Jackson Laboratory (Bar Harbor, ME) (stock number 013590) and crossed to the *Fzd6$^{-/-}$* background (Guo et al., 2004). To induce melanoma formation, we applied about 2–5 μl of 4-hydroxytamoxifen and 10 mg/ml in corn oil onto the skin (paws, ears, and tail base) of mice aged 4–5 weeks for 3 consecutive days. Mice were monitored several times a week for tumor development and progression. Mice were handled and housed according to the approved Institutional Animal Care and Use Committee protocol M006110 of the University of Wisconsin-Madison (Madison, WI).

Histological analysis

Melanoma tissue microarray was purchased from US Biomax (number ME1004g). After dewaxing and antigen retrieval, FZD6 immunostaining was carried out with the goat anti-FZD6 antibody (AF3149, 1:100, R&D Systems, Minneapolis, MN) and the VEC-TASTAIN ABC-AP Staining Kit (alkaline phosphatase, Rabbit IgG) following the manufacturer's instructions. Mouse tissues were collected and fixed in 4% formaldehyde overnight, embedded in paraffin wax, and sectioned at 4 μm. After dewaxing, the sections were stained with H&E for histological analyses. The tissue sectioning and H&E staining were performed using the services provided by the University of Wisconsin-Madison Research Animal Resources Center. Images for immunohistochemistry and H&E staining were captured using an EVOS XL Core Cell Imaging System (Thermo Fisher Scientific, Waltham, MA).

Cell culture

Human melanoma cell lines (A375, G361, Hs294T, and SK-Mel28) were obtained from ATCC (Manassas, VA) and maintained in specified media (Corning, Corning, NY) supplemented with 10% fetal bovine serum and 1% penicillin/streptomycin (Thermo Fisher Scientific) in a humidified chamber with 5% carbon dioxide at 37 °C. A375 and Hs294T were maintained in DMEM, SK-Mel28 was maintained in MEM, and G361 was maintained in McCoy's 5A medium. Nontransformed immortalized primary human melanocyte cell line (MEL-ST) was generously provided by Robert Weinberg (Whitehead Institute, Cambridge, MA). RNA and protein lysates of normal human epidermal melanocytes and melanoma cell lines 451Lu, WM35, and WM115 were provided by Nihal Ahmad's laboratory. ON-TARGETplus small interfering RNAs against various genes were purchased from Dharmacon (Lafayette, CO). Those include *FZD6*

(L-005505-00-0005), *WNT5A* (L-003939-00-0005), and *WNT10B* (L-007759-00-0005). ON-TARGETplus Nontargeting Pool (D-001810-10-05) was used as a control. Cells were transfected using the Lipofectamine RNAi-MAX (Invitrogen, Waltham, MA). FZD6 expression plasmid was generated by cloning the coding sequence of human *FZD6* from SK-MEL28 cDNA into the pRK5 vector and verified by sequencing. For all mammalian cell transfections, cells were incubated 48 hours after transfection before assaying for protein/mRNA expression unless otherwise specified. *FZD6*-KO A375 cell lines were generated using a previously described CRISPR/Cas9 approach (Ran et al., 2013). Two single-guide RNA sequences (TGACCAGAGTATTGCCGCGGTGG and CTGCTTGTTCACCCGGTTTCAGG) were designed and transfected simultaneously into cells to increase the efficiency of gene disruption. KO cell lines were established by FACS followed by screening with western blot. Cell proliferation assay was performed in 96-well plates using the CellTiter 96 AQ_{ueous} One Solution Cell Proliferation Assay Kit (Promega, Madison, WI). A total of 5,000 cells were seeded into each well, and a replicate of eight was used for each data point. For cell cycle analysis, melanoma cells were collected, washed, and fixed in 70% ethanol overnight. RNA was removed with RNase A treatment (Sigma-Aldrich, St. Louis, MO) at 37 °C for 30 minutes, and then cells were resuspended in 0.5 ml of PBS and stained with 50 μg/ml propidium iodide (Sigma-Aldrich) and subjected to Attune flow cytometer (Thermo Fisher Scientific) and analyzed with Modfit software. Matrigel invasion assay was performed using the Corning Matrigel Invasion Chambers (number 354480). In this assay, 25,000 tumor cells were resuspended with serum-free media and seeded to the Matrigel-coated top chamber (serum-containing media in the lower chamber as a chemoattractant). After 24 hours of incubation, cells that had migrated through the Matrigel and membrane were fixed and stained with an H&E Staining Kit (H-3502, Vector Laboratories, Newark, CA). A spheroid invasion assay was performed using a previously described method (Vinci et al., 2015). Briefly, 8,000 cells were seeded to 96-well round bottom plates to grow for 3 days for spheroid formation. A total of 2 mg/ml type I collagen was used as an embedding matrix. Spheroids were monitored and imaged for 2–3 days using an EVOS XL Core Cell Imaging System (Thermo Fisher Scientific).

Western blot analysis, RT-PCR, and real-time PCR

The methodologies can be found in the Supplementary Materials and Methods.

Statistical analysis

Statistical analyses were performed with two-tailed unpaired Student's *t*-test between two experimental groups and one-way ANOVA for more than two experimental groups followed by Dunnett's or Tukey's test for multiple comparisons using the GraphPad Prism 8 (GraphPad Software, San Diego, CA). A $P < 0.05$ was considered significant.

Supplementary Material

Refer to Web version on PubMed Central for supplementary material.

ACKNOWLEDGMENTS

The work was supported by grants from the National Institutes of Health (the Skin Diseases Research Center Core grant P30AR066524 and the University of Wisconsin Carbone Cancer Center Support grant P30 CA014520). HC was supported by the Department of Veterans Affairs VA Merit Review Awards I01CX002308 and the Gary S. Wood Dermatology Research Bascom Endowed Professorship. NA was supported by the Department of Veterans Affairs VA Merit Review Awards I01 BX004221 and I01 CX002210 and a Research Career Scientist Award IK6 BX003780.

Data availability statement

There is no additional data related to this article.

Abbreviations:

EMT	epithelial-mesenchymal transition
KO	knockout
PCP	planar cell polarity
PKC	protein kinase C

REFERENCES

Brabletz T, Kalluri R, Nieto MA, Weinberg RA. EMT in cancer. Nat Rev Cancer 2018;18:128–34. [PubMed: 29326430]

Caramel J, Papadogeorgakis E, Hill L, Browne GJ, Richard G, Wierinckx A, et al. A switch in the expression of embryonic EMT-inducers drives the development of malignant melanoma. Cancer Cell 2013;24:466–80. [PubMed: 24075834]

Corda G, Sala G, Lattanzio R, Iezzi M, Sallese M, Fragassi G, et al. Functional and prognostic significance of the genomic amplification of frizzled 6 (FZD6) in breast cancer. J Pathol 2017;241:350–61. [PubMed: 27859262]

Damsky WE, Curley DP, Santhanakrishnan M, Rosenbaum LE, Platt JT, Gould Rothberg BE, et al. β-catenin signaling controls metastasis in Braf-activated Pten-deficient melanomas. Cancer Cell 2011;20:741–54. [PubMed: 22172720]

Dankort D, Curley DP, Cartlidge RA, Nelson B, Karnezis AN, Damsky WE, et al. Braf(V600E) cooperates with Pten loss to induce metastatic melanoma. Nat Genet 2009;41:544–52. [PubMed: 19282848]

Daulat AM, Borg JP. Wnt/planar cell polarity signaling: new opportunities for cancer treatment. Trends Cancer 2017;3:113–25. [PubMed: 28718442]

Davey CF, Moens CB. Planar cell polarity in moving cells: think globally, act locally. Development 2017;144:187–200. [PubMed: 28096212]

Dong B, Vold S, Olvera-Jaramillo C, Chang H. Functional redundancy of frizzled 3 and frizzled 6 in planar cell polarity control of mouse hair follicles. Development 2018;145:dev168468.

Goodrich LV, Strutt D. Principles of planar polarity in animal development. Development 2011;138:1877–92. [PubMed: 21521735]

Guo N, Hawkins C, Nathans J. Frizzled6 controls hair patterning in mice. Proc Natl Acad Sci USA 2004;101:9277–81. [PubMed: 15169958]

Hanahan D, Weinberg RA. Hallmarks of cancer: the next generation. Cell 2011;144:646–74. [PubMed: 21376230]

Larkin J, Ascierto PA, Dréno B, Atkinson V, Liszkay G, Maio M, et al. Combined vemurafenib and cobimetinib in BRAF-mutated melanoma. N Engl J Med 2014;371:1867–76. [PubMed: 25265494]

Li C, Nguyen V, Clark KN, Zahed T, Sharkas S, Filipp FV, et al. Down-regulation of FZD3 receptor suppresses growth and metastasis of human melanoma independently of canonical WNT signaling. Proc Natl Acad Sci USA 2019;116:4548–57. [PubMed: 30792348]

Luga V, Zhang L, Viloria-Petit AM, Ogunjimi AA, Inanlou MR, Chiu E, et al. Exosomes mediate stromal mobilization of autocrine Wnt-PCP signaling in breast cancer cell migration. Cell 2012;151:1542–56. [PubMed: 23260141]

MacDonald BT, Tamai K, He X. Wnt/beta-catenin signaling: components, mechanisms, and diseases. Dev Cell 2009;17:9–26. [PubMed: 19619488]

Marconcini R, Spagnolo F, Stucci LS, Ribero S, Marra E, Rosa F, et al. Current status and perspectives in immunotherapy for metastatic melanoma. Oncotarget 2018;9:12452–70. [PubMed: 29552325]

Mikels AJ, Nusse R. Purified Wnt5a protein activates or inhibits beta-catenin-TCF signaling depending on receptor context. PLoS Biol 2006;4:e115. [PubMed: 16602827]

Nusse R, Clevers H. Wnt/β-catenin signaling, disease, and emerging therapeutic modalities. Cell 2017;169:985–99. [PubMed: 28575679]

Ran FA, Hsu PD, Wright J, Agarwala V, Scott DA, Zhang F. Genome engineering using the CRISPR-Cas9 system. Nat Protoc 2013;8:2281–308. [PubMed: 24157548]

Robert C, Schachter J, Long GV, Arance A, Grob JJ, Mortier L, et al. Pembrolizumab versus ipilimumab in Advanced Melanoma. N Engl J Med 2015;372:2521–32. [PubMed: 25891173]

Russo I, Zorzetto L, Chiarion Sileni V, Alaibac M. Cutaneous side effects of targeted therapy and immunotherapy for advanced melanoma. Scientifica (Cairo) 2018;2018:5036213.

Siemers NO, Holloway JL, Chang H, Chasalow SD, Ross-MacDonald PB, Voliva CF, et al. Genome-wide association analysis identifies genetic correlates of immune infiltrates in solid tumors. PLoS One 2017;12: e0179726.

VanderVorst K, Dreyer CA, Konopelski SE, Lee H, Ho HH, Carraway KL. Wnt/PCP signaling contribution to carcinoma collective cell migration and metastasis. Cancer Res 2019;79:1719–29. [PubMed: 30952630]

VanderVorst K, Hatakeyama J, Berg A, Lee H, Carraway KL. Cellular and molecular mechanisms underlying planar cell polarity pathway contributions to cancer malignancy. Semin Cell Dev Biol 2018;81:78–87. [PubMed: 29107170]

Vinci M, Box C, Eccles SA. Three-dimensional (3D) tumor spheroid invasion assay. J Vis Exp 2015;99:e52686.

Wang Y, Chang H, Rattner A, Nathans J. Frizzled receptors in development and disease. Curr Top Dev Biol 2016a;117:113–39. [PubMed: 26969975]

Wang Y, Guo N, Nathans J. The role of Frizzled3 and Frizzled6 in neural tube closure and in the planar polarity of inner-ear sensory hair cells. J Neurosci 2006;26:2147–56. [PubMed: 16495441]

Wang Y, Williams J, Rattner A, Wu S, Bassuk AG, Goffinet AM, et al. Patterning of papillae on the mouse tongue: a system for the quantitative assessment of planar cell polarity signaling. Dev Biol 2016b;419:298–310. [PubMed: 27612405]

Weeraratna AT, Jiang Y, Hostetter G, Rosenblatt K, Duray P, Bittner M, et al. Wnt5a signaling directly affects cell motility and invasion of metastatic melanoma. Cancer Cell 2002;1:279–88. [PubMed: 12086864]

White RM, Zon LI. Melanocytes in development, regeneration, and cancer. Cell Stem Cell 2008;3:242–52. [PubMed: 18786412]

Xu Q, Wang Y, Dabdoub A, Smallwood PM, Williams J, Woods C, et al. Vascular development in the retina and inner ear: control by Norrin and Frizzled-4, a high-affinity ligand-receptor pair. Cell 2004;116:883–95. [PubMed: 15035989]

Yu H, Ye X, Guo N, Nathans J. Frizzled 2 and frizzled 7 function redundantly in convergent extension and closure of the ventricular septum and palate: evidence for a network of interacting genes. Development 2012;139:4383–94. [PubMed: 23095888]

Zhai Y, Haresi AJ, Huang L, Lang D. Differences in tumor initiation and progression of melanoma in the $Braf^{CA}$;Tyr-CreERT2;$Pten^{f/f}$ model between male and female mice. Pigment Cell Melanoma Res 2020;33:119–21. [PubMed: 31449725]

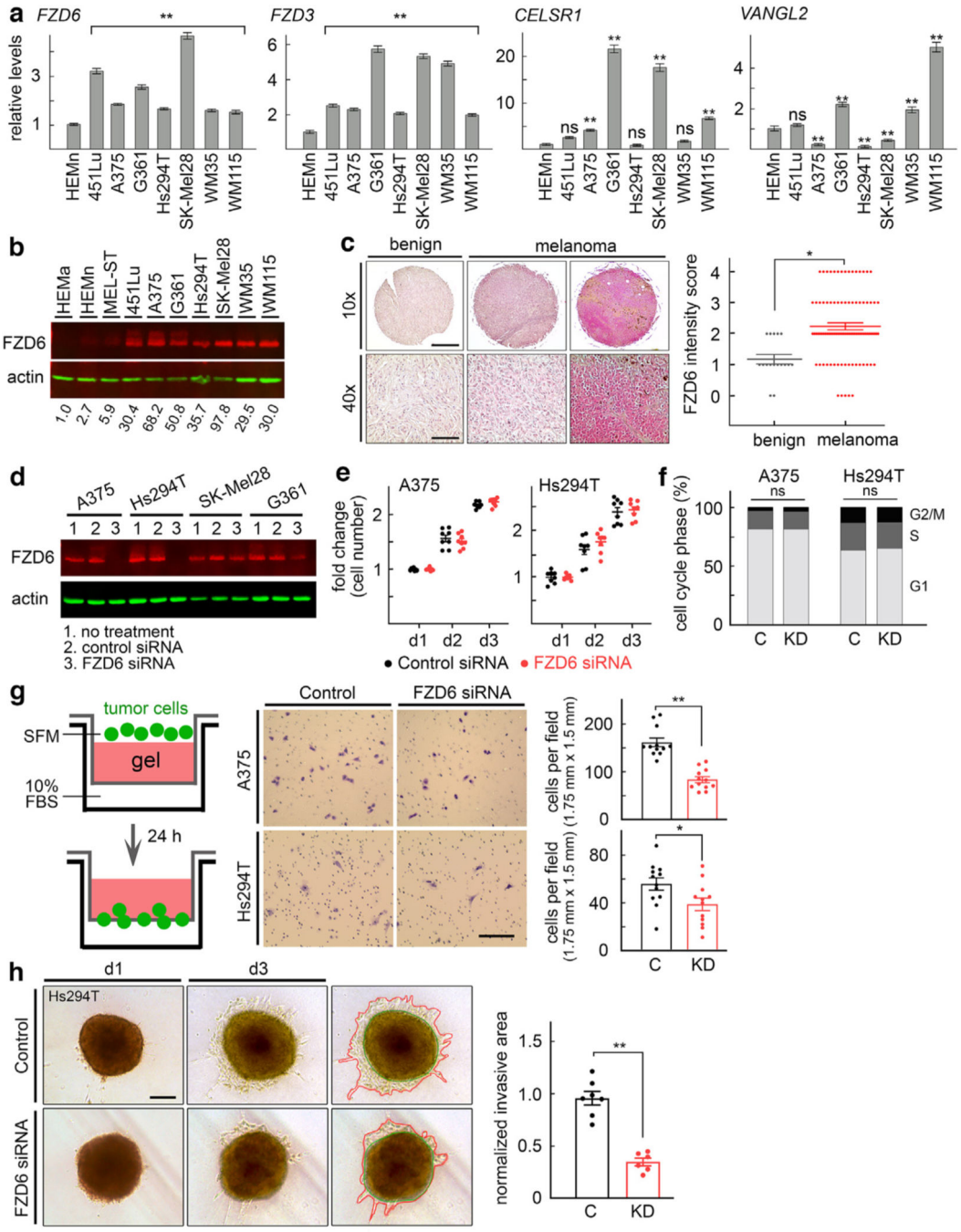

Figure 1. Effects of *FZD6* knockdown on cell proliferation and invasion.

(**a**) qRT-PCR showing misregulated expression of core PCP genes in melanoma cell lines. (**b**) High FZD6 protein levels in melanoma cells. Numbers refer to the relative level compared with adult HEMas. (**c**) FZD6 immunostaining in melanoma TMA. Bars = 400 μm in ×10 and 100 μm in ×40. (**d**) Effective knockdown of FZD6 in A375 and Hs294T cells. (**e**) *FZD6* knockdown did not affect cell proliferation. (**f**) Cell cycle distribution after *FZD6* knockdown. (**g**) Matrigel invasion assay showing reduced cell invasion after *FZD6* knockdown. (**h**) Spheroids assay showing reduced cell invasion after *FZD6* knockdown in

Hs294T cells. Bar = 200 μm for **g** and **h**. C denotes control siRNA, and KD denotes FZD6 siRNA. *$P < 0.05$ and **$P < 0.01$. d, day; FBS, fetal bovine serum; HEMa, adult human epidermal melanocyte; HEMn, newborn human epidermal melanocyte; ns, not significant; PCP, planar cell polarity; siRNA, small interfering RNA; TMA, tissue microarray.

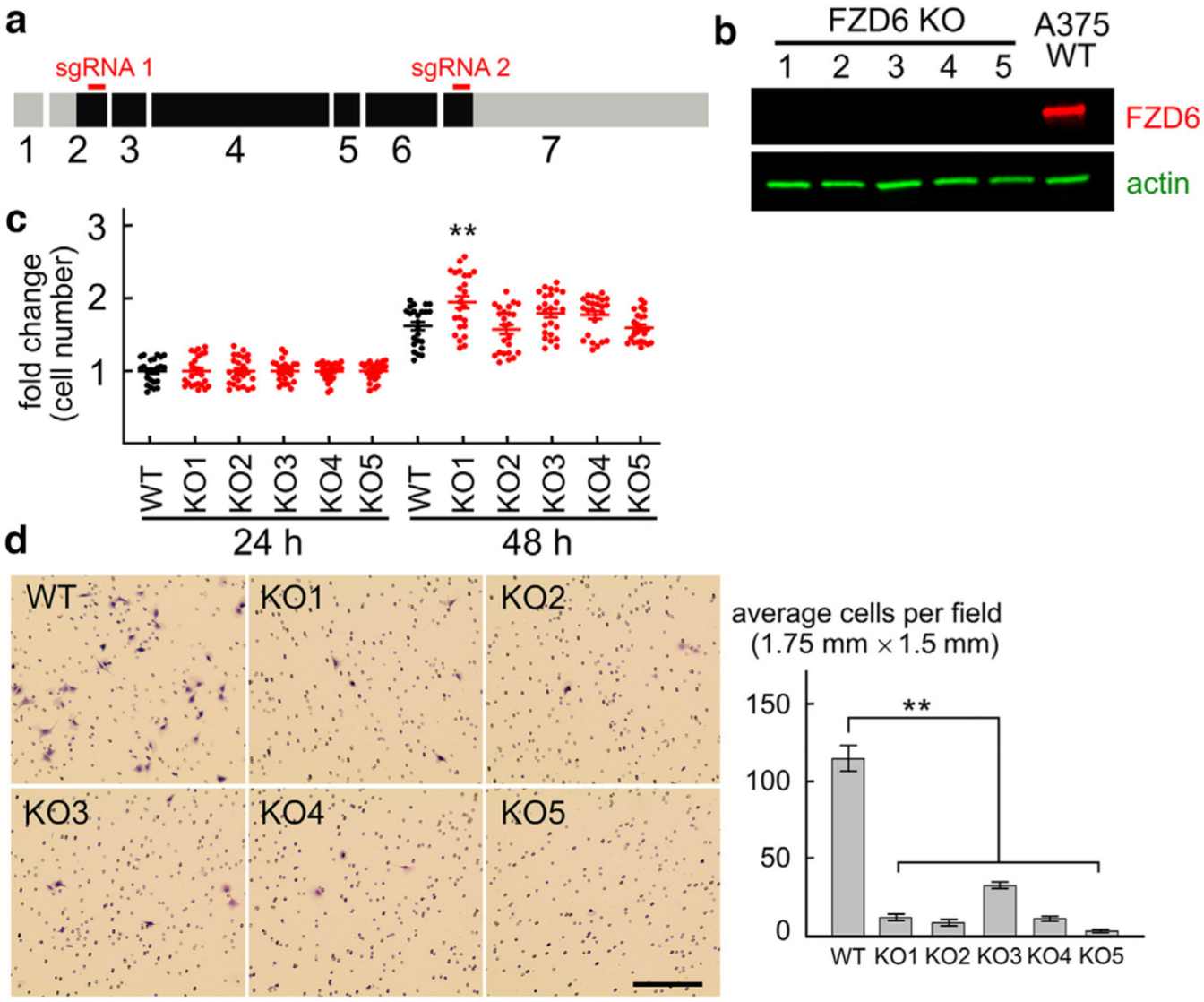

Figure 2. *FZD6* knockout inhibits cell invasion in A375 melanoma cells.

(**a**) Diagram of the human *FZD6* gene structure. Two sgRNAs were designed to target exons 2 and 7. (**b**) Western blot showing that FZD6 expression was abolished in all five selected knockout clones. Actin was used as a loading control. (**c**) Proliferation potential of *FZD6*-knockout cells. Four of five *FZD6*-knockout clones showed comparable proliferation speed as control cells. Knockout clone 1 showed a slightly increased proliferation speed. (**d**) Matrigel invasion assay showing a significant reduction of cell invasiveness in *FZD6*-knockout A375 cells. Bar = 200 μm. $^{**}P < 0.01$. KO, knockout; sgRNA, single-guide RNA; WT, wild type.

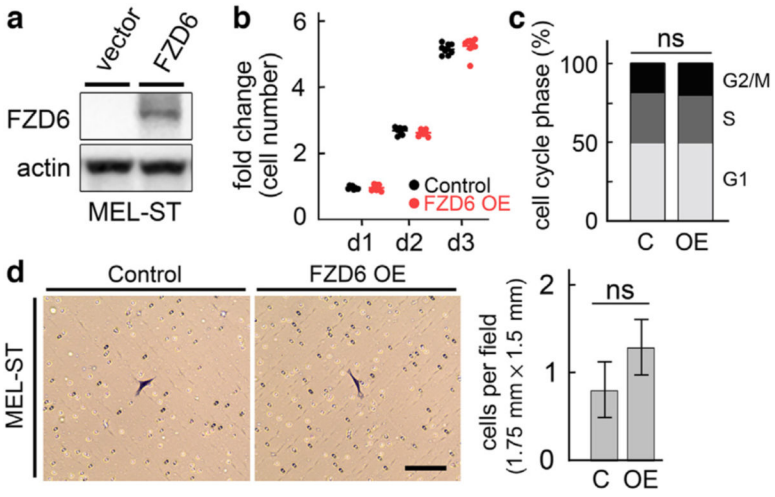

Figure 3. Effects of *FZD6* overexpression on cell proliferation and invasion in MEL-ST melanocytes.

(**a**) Western blot showing that FZD6 expression was significantly increased in MEL-ST cells transfected with *FZD6* expression plasmids. Actin was used as a loading control. (**b**) *FZD6* overexpression did not affect cell proliferation, as assessed using the CellTiter 96 AQ_{ueous} One Solution cell proliferation assay. (**c**) MEL-ST cells were analyzed for cell cycle distribution using FACS analysis after *FZD6* overexpression. (**d**) Matrigel invasion assay showing limited cell invasive capacity in MEL-ST cells and no changes upon *FZD6* overexpression. Bar = 100 μm. C denotes cells transfected with empty pRK5 vector plasmids, and OE denotes cells transfected with *FZD6* expression plasmids. d, day; ns, not significant.

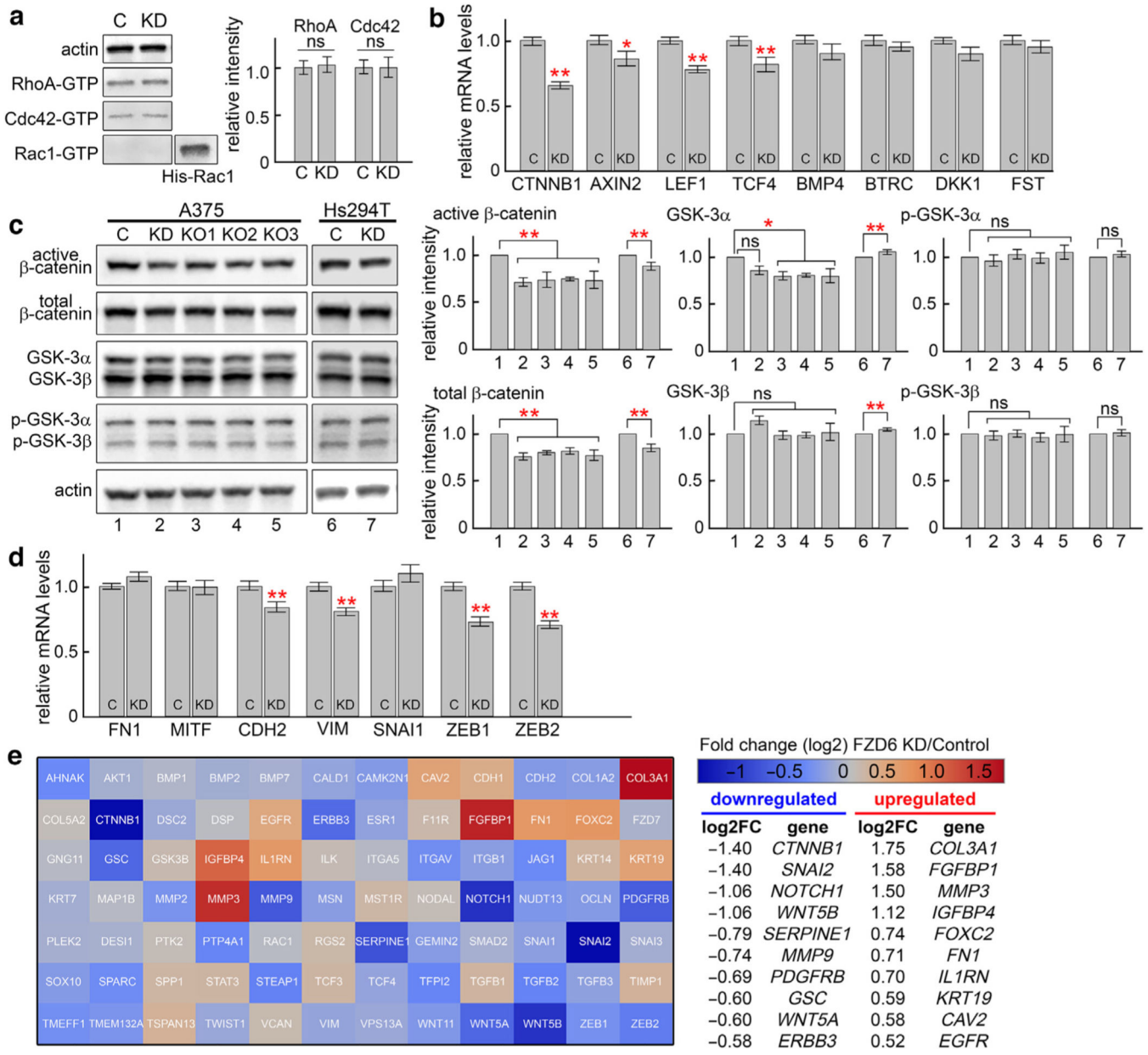

Figure 4. FZD6 regulates canonical Wnt and EMT signaling pathways in melanoma cells.

(**a**) Activation of RhoA and Cdc42 remained unchanged in A375 cells upon *FZD6* knockdown. No activated Rac1 was detected. (**b**) Expression of canonical Wnt signaling pathway genes, as assessed by qRT-PCR. (**c**) Western blot showing decreased levels of active and total β-catenin proteins upon FZD6 knockdown/knockout. GSK activity was assessed by examining the total and phosphorylated GSK-α/β. (**d**) Expression of EMT genes assessed by qRT-PCR. (e) Qiagen RT^2 Profiler PCR Array showing the effects of *FZD6* knockdown on EMT. Left: heatmap showing upregulated genes (red) and downregulated genes (blue). Right: lists showing the top 10 genes with the greatest fold change. C denotes control siRNA, KD denotes FZD6 siRNA, and KO denotes FZD6 knockout. *$P < 0.05$ and **$P < 0.01$. EMT, epithelial-mesenchymal transition; GSK, glycogen synthase kinase; ns,

not significant; p-GSK, phosphorylated glycogen synthase kinase; siRNA, small interfering RNA.

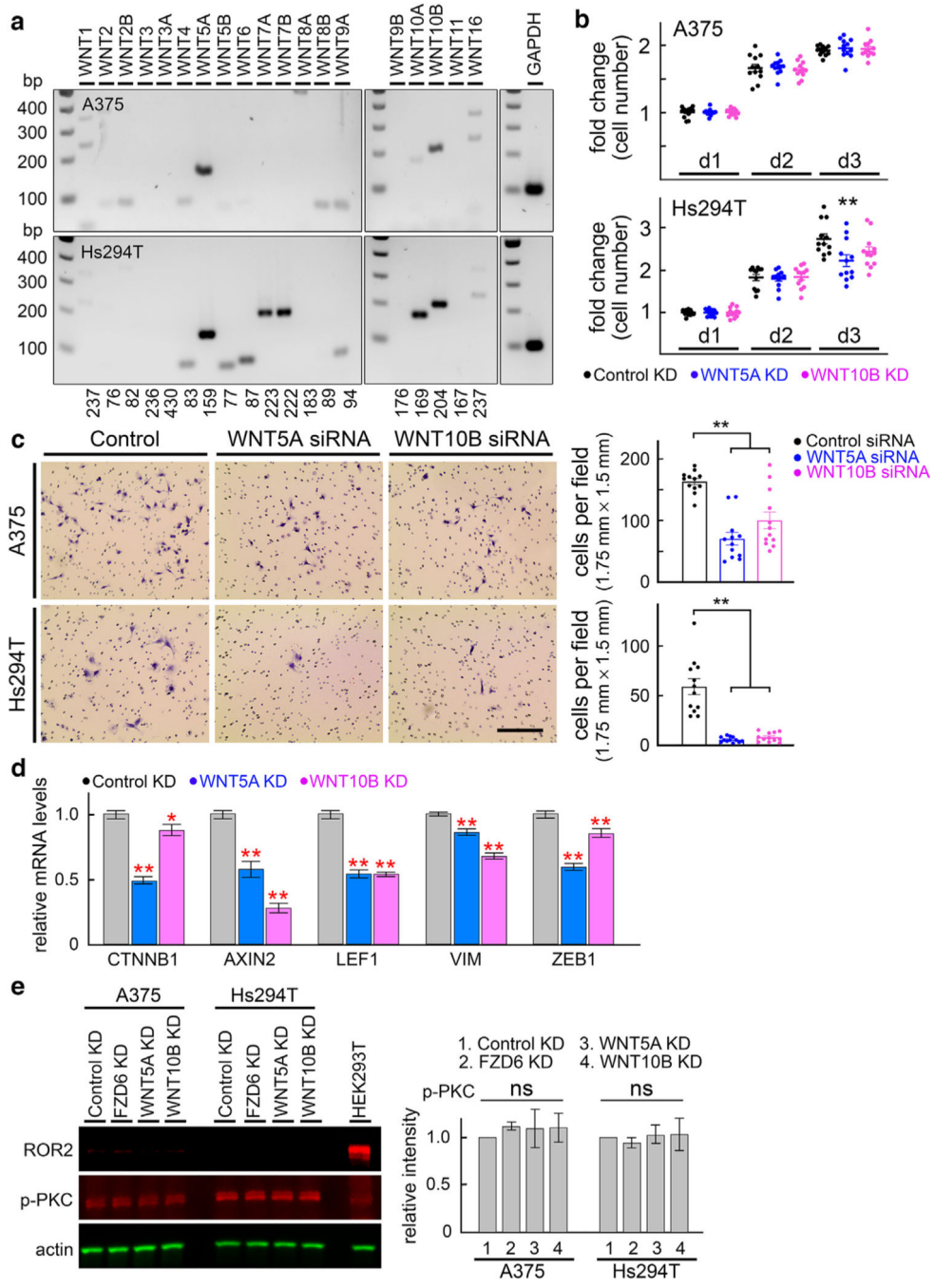

Figure 5. WNT5A and WNT10B promote cell invasion in melanoma cells.

(**a**) Expression of 19 *WNTs* in A375 and Hs294T cells, as assessed by RT-PCR. Numbers refer to the size of PCR products. (**b**) *WNT5A* knockdown reduced cell proliferation in Hs294T cells on day 3 but not in A375 cells. *WNT10B* knockdown did not affect cell proliferation. (**c**) Matrigel invasion assay showing reduced cell invasion upon *WNT5A* and *WNT10B* knockdown. Bar = 200 μm. (**d**) *WNT5A/10B*-knockdown cells shared similar changes in the expression of canonical Wnt-target genes and EMT markers with *FZD6* knockdown cells, as assessed by qRT-PCR. (**e**) Western blot showing low/no expression of

ROR2 and unchanged levels of phosphorylated PKC upon *FZD6*, *WNT5A*, and *WNT10B* knockdown. *$P < 0.05$ and **$P < 0.01$. d, day; EMT, epithelial-mesenchymal transition; KD, knockdown; ns, not significant; PKC, protein kinase C; p-PKC, phosphorylated protein kinase C; siRNA, small interfering RNA.

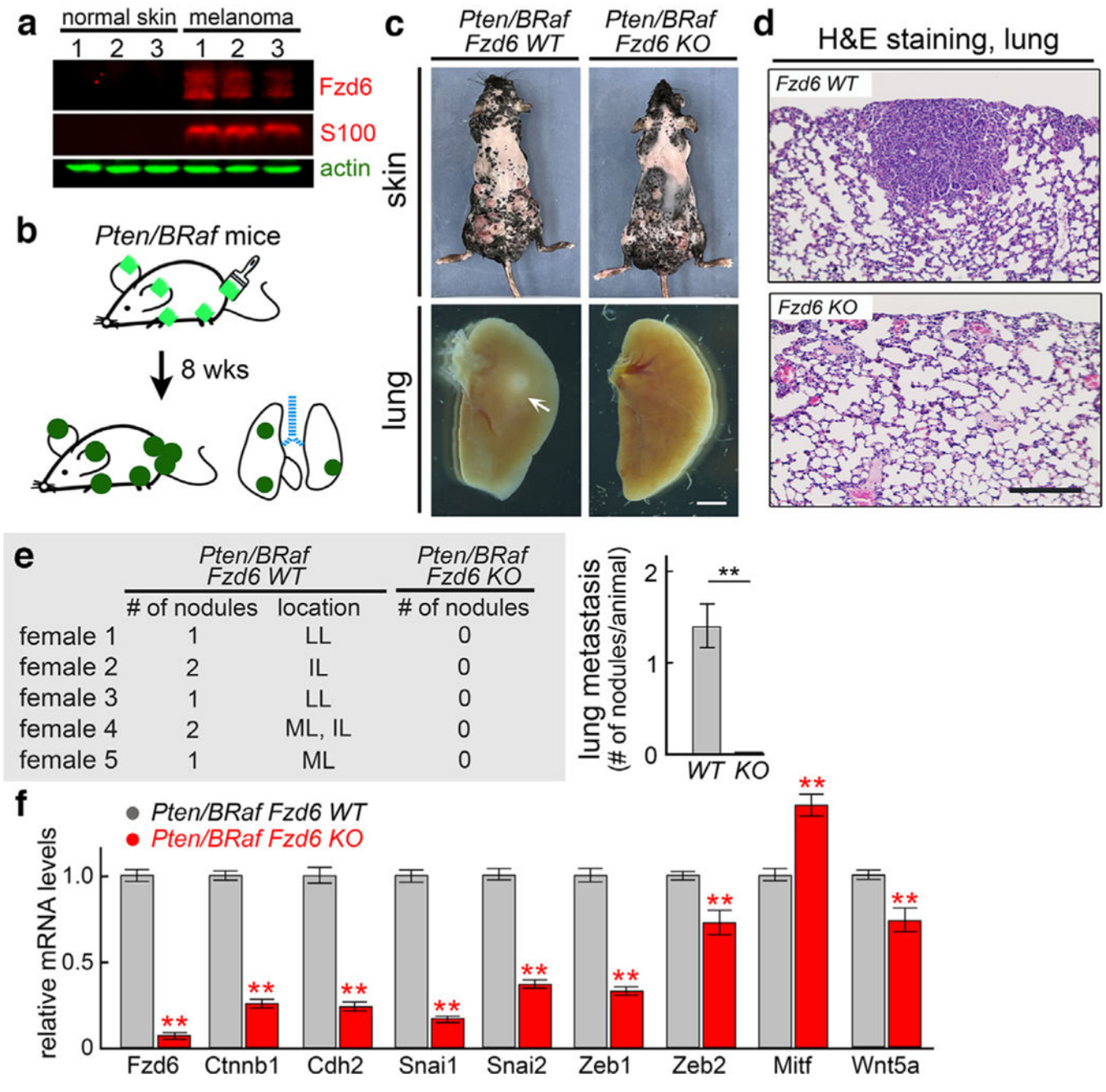

Figure 6. FZD6 is required for distant melanoma metastasis into the lung in vivo.

(**a**) Upregulated FZD6 expression in the *Pten/BRaf* melanomas. S100 is a marker for melanocytes and melanoma cells. (**b**) Diagram showing the experimental design. (**c**) Knockout of *Fzd6* did not affect primary tumor formation but inhibited distant metastasis of the melanoma into the lung. The arrow pointing to a metastatic tumor nodule in the *Pten/BRaf Fzd6* WT lung. Bar = 2 mm. (**d**) H&E staining of lung sections showing metastatic lesions in the *Pten/BRaf Fzd6* WT mice. Bar = 200 μm. (**e**) Quantification of lung metastases. LL denotes the left lung, IL denotes inferior lobe of the right lung, and ML denotes middle lobe of the right lung. (**f**) Expression of canonical Wnt signaling pathway

genes and EMT markers in primary tumors, as assessed by qRT-PCR. $^{**}P < 0.01$. EMT, epithelial-mesenchymal transition; KO, knockout; WT, wild type.